PROCEEDINGS OF SPIE

SPIEDigitalLibrary.org/conference-proceedings-of-spie

# Dark energy survey operations: years 4 and 5

H. T. Diehl, E. Neilsen, R. A. Gruendl, T. M. C. Abbott, S. Allam, et al.

H. T. Diehl, E. Neilsen, R. A. Gruendl, T. M. C. Abbott, S. Allam, O. Alvarez, J. Annis, E. Balbinot, S. Bhargava, K. Bechtol, G. M. Bernstein, R. Bhatawdekar, S. Bocquet, D. Brout, R. Capasso, R. Cawthon, C. Chang, E. Cook, C. J. Conselice, J. Cruz, C. D'Andrea, L. da Costa, R. Das, D. L. DePoy, A. Drlica-Wagner, A. Elliott, S. W. Everett, J. Frieman, A. Fausti Neto, A. Ferté, I. Friswell, K. E. Furnell, L. Gelman, D. W. Gerdes, M. S. S. Gill, D. A. Goldstein, D. Gruen, D. J. Gulledge, S. Hamilton, D. Hollowood, K. Honscheid, D. J. James, M. D. Johnson, M. W. G. Johnson, S. Kent, R. S. Kessler, G. Khullar, E. Kovacs, A. Kremin, R. Kron, N. Kuropatkin, J. Lasker, A. Lathrop, T. S. Li, M. Manera, M. March, J. L. Marshall, M. Medford, F. Menanteau, I. Mohammed, M. Monroy, B. Moraes, E. Morganson, J. Muir, M. Murphy, B. Nord, A. B. Pace, A. Palmese, Y. Park, F. Paz-Chinchón, M. E. S. Pereira, D. Petravick, A. A. Plazas, J. Poh, T. Prochaska, A. K. Romer, K. Reil, A. Roodman, M. Sako, M. Sauseda, D. Scolnic, L. F. Secco, I. Sevilla-Noarbe, N. Shipp, J. A. Smith, M Soares-Santos, B. Soergel, A. Stebbins, K. T. Story, K. Stringer, F. Tarsitano, B. Thomas, D. L. Tucker, K. Vivas, A. R. Walker, M.-Y. Wang, C. Weaverdyck, N. Weaverdyck, W. Wester, C. F. Wethers, R. Wilkenson, H.-Y Wu, B. Yanny, A. Zenteno, Y. Zhang, "Dark energy survey operations: years 4 and 5," Proc. SPIE 10704, Observatory Operations: Strategies, Processes, and Systems VII, 107040D (10 July 2018); doi: 10.1117/12.2312113

SPIE.

Event: SPIE Astronomical Telescopes + Instrumentation, 2018, Austin, Texas, United States

# The Dark Energy Survey and Operations: Years 4 and 5

H. T. Diehl[1a], E. Neilsen[a], R. A. Gruendl[b,c], T. M. C. Abbott[d], S. Allam[a], O. Alvarez[a], J. Annis[a], E. Balbinot[e], S. Bhargava[f], K. Bechtol[g], G. M. Bernstein[h], R. Bhatawdekar[i], S. Bocquet[j,k], D. Brout[h], R. Capasso[k,l], R. Cawthon[m,n], C. Chang[m], E. Cook[o], C. J. Conselice[i], J. Cruz[d], C. D'Andrea[h], L. da Costa[p], R. Das[q], D. L. DePoy[o], A. Drlica-Wagner[a], A. Elliott[r], S. W. Everett[s], J. Frieman[a,m,n], A. Fausti Neto[p], A. Ferté[t], I. Friswell[t], K. E. Furnell[u], L. Gelman[b], D. W. Gerdes[q], M. S. S. Gill[v], D. A. Goldstein[w,x], D. Gruen[y,v], D. J. Gulledge[z], S. Hamilton[q], D. Hollowood[s], K. Honscheid[r,aa], D. J. James[d,ab], M. D. Johnson[b], M. W. G. Johnson[b], S. Kent[a], R. Kessler[m], G. Khullar[m,n], E. Kovacs[j], A. Kremin[q], R. Kron[a], N. Kuropatkin[a], J. Lasker[m,n], A. Lathrop[a], T. S. Li[a], M. Manera[ac], M. March[h], J. L. Marshall[o], M. Medford[w,x], F. Menanteau[b,c], I. Mohammed[a], M. R. Monroy[ad], B. Moraes[ac], E. P. Morganson[b,c], J. Muir[q], M. Murphy[a], B. Nord[a], A. B. Pace[o], A. Palmese[ac], Y. Park[ae], F. Paz-Chinchón[b], M. E. S. Pereira[af], D. Petravick[b], A. A. Plazas[ag], J. Poh[m,n], T. Prochaska[o], K. Reil[y,v], A. K. Romer[f], A. Roodman[y,v], M. Sako[h], M. Sauseda[o], D. Scolnic[m], L. F. Secco[h], I. Sevilla-Noarbe[ad], N. Shipp[m,n], J. A. Smith[z], M. Soares-Santos[a,af], B. Soergel[ah], A. Stebbins[a], K. T. Story[y,v], K. Stringer[o], F. Tarsitano[ai], B. Thomas[aj], D. L. Tucker[a], A. K. Vivas[d], A. R. Walker[d], M.-Y. Wang[o], C. Weaverdyck[q], N. Weaverdyck[q], W. Wester[a], C. F. Wethers[ak], R. Wilkinson[f], H.-Y. Wu[r], B. Yanny[a], A. Zenteno[d], Y. Zhang[a]

[a]Fermi National Accelerator Laboratory, P.O. Box 500, Batavia, IL 60510, USA; [b]National Center for Supercomputing Applications, 1205 West Clark St., Urbana, IL 61801, USA; [c]Department of Astronomy, University of Illinois at Urbana-Champaign, W. Green Street, Urbana, IL 61801, USA; [d]National Optical Astronomy Observatory, Cerro Tololo Inter-American Observatory, Casilla 603, La Serena, Chile; [e]Department of Physics, University of Surrey, Guildford GU2 7XH, UK; [f]Department of Physics and Astronomy, Sussex, UK; [g]LSST, 933 North Cherry Avenue, Tucson, AZ 85721, USA; [h]Department of Physics and Astronomy, University of Pennsylvania, Philadelphia, PA 19104, USA; [i]School of Physics and Astronomy, University of Nottingham, University Park, Nottingham, NG7 2RD, UK; [j]Argonne National Laboratory, 9700 South Cass Ave., Lemont, IL 60439, USA; [k]University Observatory Munich, Scheinerstrasse 1, 81679 Munich, Germany; [l]Excellence Cluster Universe, 85748 Garching b. Munich, Germany; [m]Kavli Institute for Cosmological Physics, University of Chicago, Chicago, IL 60637, USA; [n]Department of Astronomy and Astrophysics, University of Chicago, Chicago, IL 60637, USA; [o]George P. and Cynthia Woods Mitchell Institute for Fundamental Physics and Astronomy, and Department of Physics and Astronomy, Texas A&M University, College Station, TX 77843, USA; [p]Laboratório Interinstitucional de e-Astronomia - LIneA, Rua Gal. José Cristino 77, Rio de Janeiro, RJ - 20921-400, Brazil; [q]Department of Physics, University of Michigan, Ann Arbor, MI 48109, USA; [r]Department of Physics, The Ohio State University, Columbus, OH 43210, USA; [s]Department of Physics and Santa Cruz Institute for Particle Physics, University of California, Santa Cruz, CA 95064, USA; [t]Institute for Astronomy, University of Edinburgh, Blackford Hill, Edinburgh EH9 3HJ, UK; [u]Astrophysics Research Institute, Liverpool John Moores University, IC2, Liverpool Science Park, 146 Brownlow Hill, Liverpool L3 5RF, UK; [v]SLAC National Accelerator Laboratory, Menlo Park, CA 94025, USA; [w]Lawrence Berkeley National Laboratory, 1 Cyclotron Road, Berkeley, CA 94720, USA;

[1] Diehl@FNAL.GOV; phone 1-630-840-8307.

Observatory Operations: Strategies, Processes, and Systems VII, edited by Alison B. Peck, Robert L. Seaman, Chris R. Benn, Proc. of SPIE Vol. 10704, 107040D · © 2018 SPIE
CCC code: 0277-786X/18/$18 · doi: 10.1117/12.2312113

[x]Department of Astronomy, University of California, Berkeley, 501 Campbell Hall, Berkeley, CA 94720, USA; [y]Kavli Institute for Particle Astrophysics and Cosmology, 452 Lomita Mall, Stanford University, Stanford, CA 94305, USA; [z]Department of Physics and Astronomy, Austin Peay State University, Clarksville, TN 37044, USA; USA; [aa]Center for Cosmology and Astro-Particle Physics, The Ohio State University, Columbus, OH 43210, USA; [ab]Harvard-Smithsonian Center for Astrophysics, Cambridge, MA 02138, USA, [ac]Department of Physics and Astronomy, University College London, Gower St., London, WC1E 6BT, UK; [ad]Centro de Investigaciones Energéticas, Medioambientales y Tecnológicas (CIEMAT), Madrid, Spain; [ae]Dept. of Physics, University of Arizona, Tucson, AZ 85721, USA; [af]Department of Physics, Brandeis University, Waltham, MA 02453, USA; [ag]Jet Propulsion Laboratory, California Institute of Technology, 4800 Oak Grove Dr., Pasadena, CA 91109, USA; [ah]Kavli Institute for Cosmology, University of Cambridge, Madingley Road, Cambridge CB3 0HA, UK; [ai]Institute for Astronomy, Department of Physics, ETH Zurich, Wolfgang-Pauli-Strasse 27, CH-8093 Zurich, Switzerland; [aj]Institute of Cosmology and Gravitation, University of Portsmouth, Portsmouth, PO1 3FX, UK; [ak]Institute of Astronomy, University of Cambridge, Madingley Road, Cambridge CB3 0HA, UK

## ABSTRACT

The Dark Energy Survey (DES) is an operating optical survey aimed at understanding the accelerating expansion of the universe using four complementary methods: weak gravitational lensing, galaxy cluster counts, baryon acoustic oscillations, and Type Ia supernovae. To perform the 5000 sq-degree wide field and 30 sq-degree supernova surveys, the DES Collaboration built the Dark Energy Camera (DECam), a 3 square-degree, 570-Megapixel CCD camera that was installed at the prime focus of the Blanco 4-meter telescope at the Cerro Tololo Inter-American Observatory (CTIO). DES has completed its third observing season out of a nominal five. This paper describes DES "Year 4" (Y4) and "Year 5" (Y5), the survey strategy, an outline of the survey operations procedures, the efficiency of operations and the causes of lost observing time. It provides details about the quality of these two-season's data, a summary of the overall status, and plans for the final survey season.

**Keywords:** Cosmology, Dark Energy Survey, Dark Energy Camera, Operations, CTIO

## 1. INTRODUCTION

The Dark Energy Survey (DES) team is an international collaboration, with over 500 scientists from 25 institutions and consortiums in the US, Chile, the UK, Spain, Brazil, Switzerland, and Germany. The DES [1] main science goal is to measure dark energy parameters using four complementary techniques: galaxy cluster counting, baryon acoustic oscillations, weak gravitational lensing, and Type Ia supernovae. A rich dataset also enables Milky Way, solar system, and a variety of other extragalactic science [2]. DES is comprised of two interleaved surveys. The wide-field (WF) survey identifies stars and galaxies, and reports shapes and magnitudes in 5 filters, in 5000 square degrees of the southern galactic cap. A transient survey repeatedly images ten 2.7-square-degree fields with the purpose of identifying Type 1a supernovae. To carry out these surveys, the DES Collaboration constructed a new instrument, the Dark Energy Camera and installed it on the Victor M. Blanco 4m telescope on Cerro Tololo in Chile during 2012. DES has been carrying out survey operations during five seasons spanning roughly mid-August to mid-February. The first such season, Y1, finished in Feb. 2014. Y3 finished in feb. 2016. Y5 finished in Feb. 2018.

### The Dark Energy Camera and Auxiliary Detectors

The Dark Energy Camera (DECam) [3] consists of a wide-field corrector, a mosaic CCD imager and associated mechanical, optical, and electronic components. The optical corrector has 5 fused-silica optical elements to attain an f/2.7, 2-degree-wide image at the focal plane. DES uses 5 filters, DES g, r, i, z, and Y-bands, with central wavelengths 473, 642, 784, 926, and 1009 nm, respectively. The focal plane itself has a 42-cm radius and is populated with 62

2048x4096 pixel 250 μm thick, fully-depleted, red-sensitive CCDs, for imaging. Figure 1 shows a photo of the Dark Energy Camera mounted at the prime focus of the Blanco telescope.

Three auxiliary detectors on the CTIO summit, supplied by DES, provide information for photometric calibration. An All-Sky Radiometric Camera (RASICAM) [5-7] is used to monitor the sky using the wavelength range 970 nm to 1250 nm. In this wavelength range, relatively warm clouds are easily distinguished from cold, clear skies. "GPSMon" [5,8] provides a cross-check of the amount of precipitable water vapor (PWV) in the atmosphere. The Atmospheric Transmission Monitoring Camera (aTmCam) [5,9-10] has been operated consistently starting at the beginning of Y2. The aTmCam consists of a Paramount telescope mount and four small telescopes, each with a different narrowband filter, which monitors the brightness of suitable standard stars, thus providing the atmospheric transmission in wavelength regions dominated by the PWV and aerosol optical depth.

*Figure 1 The Dark Energy Camera is mounted at the prime focus of the Blanco 4m telescope at CTIO. The covers for the primary mirror are open. The camera assembly, including the support cage, is approximately 3.6 m long and is secured to the inner telescope ring. The camera, not including the support cage and counterweights, weighs approximately 4350 kg. Subsequent to the date of this photo, the cage was retrofitted with aluminum side-covers. The aluminum covers of two of the four readout electronics crates are visible near the top of the camera, just underneath the "Top Cap".*

**The Dark Energy Survey Fields & Footprint**

The 5000 square-degree WF survey has three main regions (see Figure 2) within the southern Galactic Cap. There is a broad roughly circular region from RA of roughly 0 to 120 degrees and DEC -70 to -10 degrees that provides a large contiguous area for the large-scale structure measurements. There is a wide roughly box-shaped region around the South Pole Telescope (SPT) observing area [11]. Finally, the survey encompasses a part of SDSS Stripe 82 [12], primarily for photometric calibration purposes. The ten 2.7 square-degree transient fields are observed with a cadence of about 7 days throughout the DES seasons, which are about ½-year long.

The footprint of a single DECam exposure is roughly hexagonal, constrained to an orientation aligned with celestial coordinates by the equatorial mount of the Blanco telescope; therefore, an area of the sky covering a particular range

of R.A. can be covered with minimal gaps and overlaps by using a hexagonal tiling pattern aligned in declination. A "tiling" is a set of exposures, one in each of 5 filters, at pointings arranged in such a pattern. Over wider ranges of R.A. the planar approximation of the sky breaks down, so the strictly hexagonal layout is "broken" every 30 degrees of R.A., resulting in extra overlaps between exposures within a tiling at 30 degree intervals. A single tiling collects useful science data on roughly 83% of the footprint area due to these breaks, deviation from the planar approximation with each 30 degree R.A. neighborhood, and incomplete coverage within each hex (due to, for example, gaps between CCDs, bad CCDs, and problematic area near the edges of the CCDs). The plan for the DES WF survey specifies 10 separate tilings, each offset from the others by a significant fraction of the camera field of view, such that observations of individual astronomical sources are spread across the focal plane. The g, r, i, and z-band exposures are 90 seconds duration. The Y-band exposures are 45 seconds duration for tilings 1-6. In Y4 we changed the Y-band observations to 90 seconds for tilings 7 and 9 and dropped tilings 8 and 10 to improve the observing duty cycle.

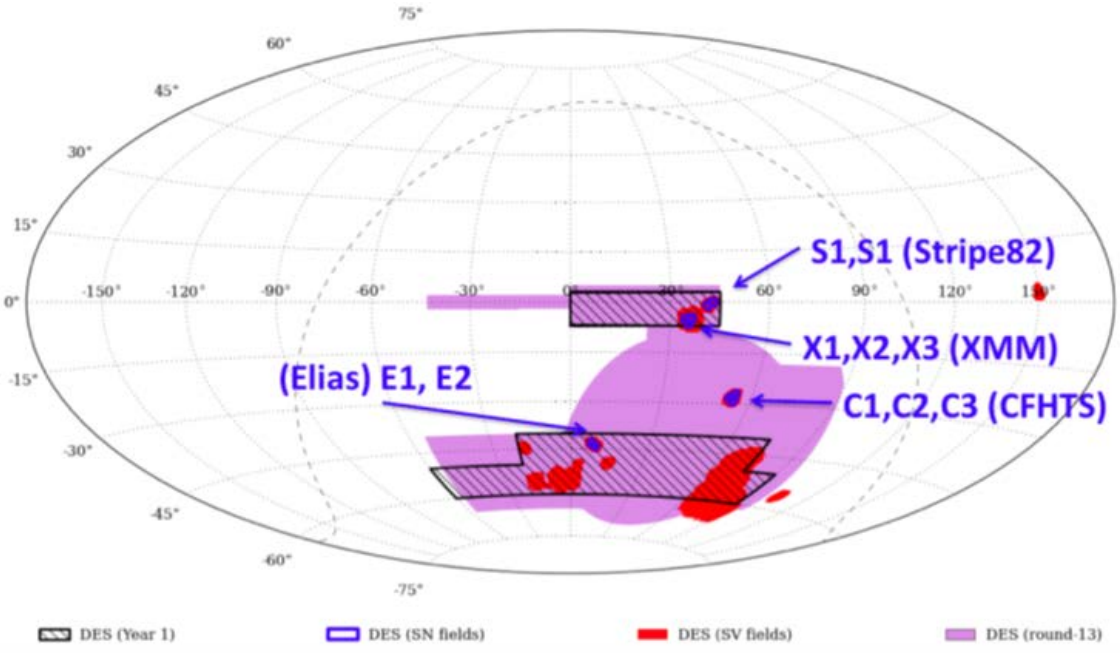


*Figure 2. The Dark Energy Survey observing "wide fields" are shown on this plot of RA and DEC. During Y1 DES observed the areas outlined in dark blue, which encompass SDSS Stripe 82 (upper) and the SPT area (lower). In Y2 we observed the complementary part of the WF. After that we aimed for two complete tilings per season. The legend also shows the Science Verification fields (red blotches), and SN fields (blue).*

*Table 1 RA and DEC (J2000) of the 10 DES supernova fields. Fields C3 and X3 are "deep fields". The other 8 fields are "shallow fields".*

| Field Name | RA | DEC |
|---|---|---|
| E1 | 7.8744 (00:31:29.9) | -43.0096 (-43:00:34.6) |
| E2 | 9.5000 (00:38:00.0) | -43.9980 (-43:59:52.8) |
| S1 | 42.8200 (02:51:16.8) | 0.0000 (00:00:00.0) |
| S2 | 41.1944 (02:44:46.7) | -0.9884 (-00:59:18.2) |
| C1 | 54.2743 (03:37:05.8) | -27.1116 (-27:06:41.8) |
| C2 | 54.2743 (03:37:05.8) | -29.0884 (-29:05:18.2) |
| C3 | 52.6484 (03:30:35.6) | -28.1000 (-28:06:00.0) |
| X1 | 34.4757 (02:17:54.2) | -4.9295 (-04:55:46.2) |
| X2 | 35.6646 (02:22:39.5) | -6.4121 (-06:24:43.6) |
| X3 | 36.4500 (02:25:48.0) | -4.6000 (-04:36:00.0) |

The time domain survey is used to identify Type Ia SNe through difference imaging [13] and measurement of the light curves. The 10 time-domain fields, shown in Table 1, are observed on a regular cadence. The 8 "shallow fields" are observed for single exposures in g-band (175s), r-band (150s), and i-band (200s) and for two images in z-band (200s each). The 5 exposures of a shallow field are considered a "sequence" and the sequence is observed consecutively. The two "deep fields" are observed for 3 exposures of 200s each in g-band, for 400s each in r-band, for 5 exposures of 360s each in i-band, and for 11 exposures of 330s each in z-band. The exposures in each given filter for the deep fields are considered a sequence. The exposures for each filter are sequential but the different filters might be observed at different times during a single night or on different nights. The limiting magnitudes [13] for difference imaging detections is about 23.5 in each band of the shallow field epochs and about 24.5 for the deep field epochs. Because the telescope pointing is accurate to only 5 to 7 arcseconds in RA and DEC, each SN sequence is preceded by a 10s "pointing" exposure that is processed to determine a correction that is applied before the first exposure in the sequence starts.

This paper describes DES "Year 4" (Y4) and "Year 5" (Y5) operations. Section 2 describes the survey procedures, Section 3, the maintenance and improvements to the camera and observing systems. Section 4, the Y4 and Y5 narrative including a description of the strategy and goals for the data-taking, the efficiency of survey operations and the progress towards the survey goals. Section 5 describes the plan and outlook for Y6, the final year of the survey.

## 2. THE DES SURVEY PROCEDURES

**Observation Schedule & Staffing**

The DES observations are staffed at the telescope by collaboration members. The Operations Scientist schedules the observing team from among the volunteers. There are three observing roles during full nights. "Observer 1" controls the camera through the data-acquisition interfaces [5] and executes the nightly program by following standard DES observing procedures [14]. This observer ensures that images are being recorded, pays attention to the alarms and warnings, and solves routine problems where procedures have been established. "Observer 2" performs quality control procedures, checks the exposures for problems and ensures that the image quality is as expected given the current conditions. The "Run Manager" is the lead observer and is responsible for ensuring that the two other observers understand how to perform their roles. Though observers are asked to read online procedures in advance of their observing trips, training is performed on site by the Run Manager. The Run Manager also has some daytime responsibilities described below, so they are not expected to stay up for the full night. During half-night observations DES usually has only two observers with the Run Manager taking on one of the roles.

Generally, the "Observer 1" and "Observer 2" roles could be performed by an inexperienced but attentive observer. We often fill those positions with people who have no previous observing experience. We required Run Managers to have mastered both of those observing roles and to have been instructed in their new duties. In practice, by the start of Y4, the observing procedures had been improved and failure probabilities reduced to the point that an attentive rookie observer could be qualified as a "Run Manager" with about 6 nights of experience.

The observing teams were assembled by the DES Operations Scientist from the list of volunteers. The duration of observing stints depended on the schedule constraints (non-observing gaps), whether the nights were full-nights or half-nights, and the preference of experienced observers. In Y4 and Y5, typical shift durations were 6 to 9 nights long. A few observers took shifts as long as 11 nights. This departed from the early DES seasons where some Run Managers observed for more than 3 weeks (with a break of a night or two in the middle). During periods where we observed for more than about ten nights in a row, we rotated-in fresh observers so that the observing teams had considerable overlap. We found that having a well-staffed and well-rested observation team reduced the chance for mistakes and misunderstandings that cost observing efficiency.

Support was available to the observers through the CTIO Telescope Operator (on hand), the CTIO Observer Support Specialist (on-site), the CTIO Instrument Scientist (typically by phone), and the DES Operations Scientist & Support Team (by internet connection). The CTIO staff handles most of the infrequent observing glitches and stops.

**Daily Operations Cycle**

The typical "Daily Cycle" starts with the Run Manager's Meeting held daily at 16:00 CTIO time. The Run Manager meets by phone with the Operations Scientist & Support and Data Management (DESDM) Teams. We discuss any technical or procedural problems that occurred during the previous night, provide additional information to DESDM about individual images that might be problematic (for example, if the telescope slewed during the image), receive the DESDM-calculated data quality from previous night's imaging, and discuss what to expect from the "Observing Tactician" (OBSTAC) (see next subsection) based on the expected weather conditions. We discuss any special procedures that the observers might need to execute, such as or special calibrations or Target-of-Opportunity (TOO) observations, including the conditions under which they are to be observed. After this meeting the Run Manager implements the data quality, updating the Exposure Table so that OBSTAC has up-to-date information on which images need to be redone.

The period before twilight is used for calibrations and to establish the basic functionality of the instrument. An LED system [15] illuminates a flat-field screen attached to the inside of the dome. We take a set of biases and flats in each of the filters. These images are used in the daily calibration. An hour before sunset the telescope operator will open the dome. At minus 10 degree twilight (roughly 40 minutes after sunset) the observers execute three standard star field [16] exposure scripts, one at high airmass (X=1.65 to 2.1), one at medium airmass (X=1.25-1.65), and one at low airmass (X<1.25). The standard star fields are fields of stars with previously calibrated brightnesses in each of the DES filter bands. They are used for characterizing that night's instrumental and atmospheric response (by fitting the observations to a set of "photometric equations") and are an integral part of the photometric calibration for DES. At minus 12 degree twilight (roughly 48 minutes after sunset) the observers begin OBSTAC observations. These continue during the night until minus 10 degree morning twilight, for standard star observations, and finally dome. Observer 1 controls SISPI and makes sure exposures are being recorded as expected. Observer 2 maintains a watch on the data quality using streamlined image analysis tools such as "Quick Reduce" [5,14] developed by DES-Brazil and KENTools [14].

The observers maintain commentary and notes in an electronic logbook. At the end of each night the observers create two night summaries. The "CTIO Night Report" lists weather conditions, problems encountered, and the fraction of time lost to each. The "DES Night Summary" provides the narrative of the shift including the expected plan with ephemeris, the conditions, accomplishments, problems encountered, and notes for the DESDM team. A series of automatically generated plots and statistics follows, including transparency, PSF, and ellipticity of stars for each image, a note of any gaps between exposures of greater than 60 seconds, the progress on wide-field and SN surveys, and a list of exposures. This summary provides a concise history of what happened during that particular night.

The images are transferred by the NOAO Data Transport System [17] (DTS) to NCSA/UIUC in Urbana-Champaign, Illinois, usually within 5 minutes after the moment that the shutter closed. Copies of the data are stored in La Serena and at the NOAO Science Archive in Tucson [18]. To conserve both disk space and network bandwidth the DECam data are losslessly FITS tile-compressed [19] using FPACK. Note that both the DESDM pipeline, described below, and the Community Pipeline [20] use a lossy FPACK compression [21].

The camera and telescope are returned to a safe condition after observations are finished.

**OBSERVING TACTICIAN (OBSTAC)**

During the course of the season a variety of weather, seeing, and sky-brightness (Moon) conditions are expected to occur. A computer application, the "Observing Tactician" (OBSTAC) [22] uses this information to select the highest priority fields to observe during the next short (5-15 minute) interval throughout the night. A simplified version of the OBSTAC decision tree is shown in Figure 3. If any of the time-domain fields have not been observed in the past 6 nights, then OBSTAC selects the field with the longest gap to minimize deviation from the desired time-domain cadence. If there are time-domain fields that have not been observed in the past 3 nights, and the seeing is too poor to take exposures useful for weak-lensing ellipticity measurements but sufficient for SN photometry, then these are observed, resetting the cadence at minimal cost to wide-survey progress. OBSTAC will then select among not yet completed wide-survey exposures (tracked by an exposure table in the SISPI database) that are likely to be of acceptable quality (based on predicted airmass, seeing, and sky brightness).

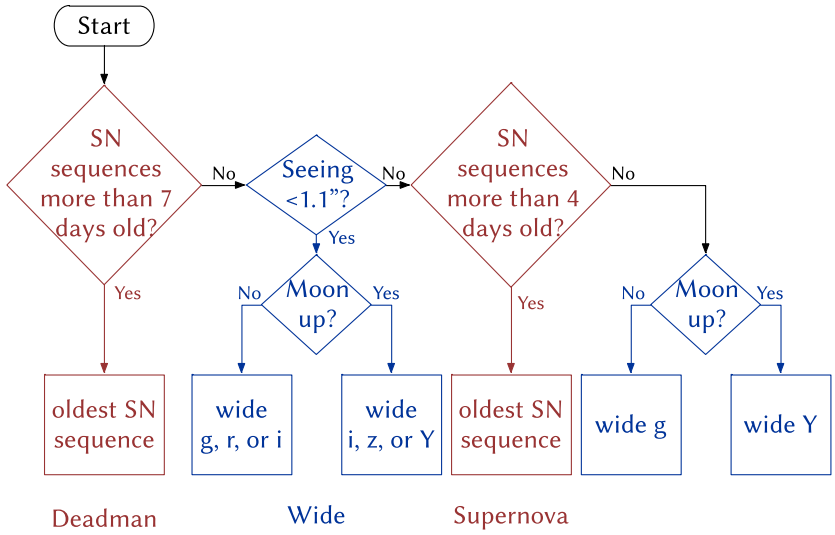


*Figure 3 A slightly simplified version of the scheduling algorithm implemented by the Observing Tactician algorithm "OBSTAC" used in Y4 and Y5. The "seeing" is that expected based on current conditions when projected to an equivalent i-band observation taken at zenith. "wide" is short for "wide-field" observations. Priorities can be adjusted for tiling #, RA & DEC, etc … in the wide field survey. From left, the horizontal choices are loosely labeled "condition 1" for "deadman SN", "condition 2" for good PSF WF, "condition 3" for poor PSF SN observations should any sequence not have been observed in the previous 4 nights, and "condition 4" if the PSF is poor and the SN are all already up-to-date.*

**Data Processing & Data Quality**

The DESDM pipeline [23] performs image detrending and calibration, that we refer to as "First Cut", in order to assess the quality of each exposure with respect to the minimum requirements necessary for DES to obtain its scientific objectives. The overscan and bias is subtracted and the image is divided by the mean dome flat. The CCD crosstalk is removed using a premeasured matrix, a linearity correction applied, fringe and pupil ghost corrections are combined, and a star flat is applied to subsections of each CCD. An astrometric solution for each image is found by comparing to known stellar positions in the 4th USNO Astrograph Catalog (UCAC-4) [24]. Finally, the point spread function (PSF) is determined by examining the shapes of stellar images and then the position, brightness, and rudimentary shape of objects detected in each image are cataloged.

We determine if the image is adequate for the wide-field survey by requiring that the "Effective Exposure Time" [25], $t_{effective}=(0.9k/FWHM)^2(Bkgd_{dark}/Bkdg)(10^{-2C/2.5})$ exceeds a minimum. Here k is a filter-dependent "Kolmogorov Factor" scaled relative to i-band that takes into account the natural seeing dependence on wavelength, FWHM is the delivered point-spread-function for stars, Bkgd and $Bkgd_{dark}$ are the measured sky background and dark sky condition, and C is the atmospheric extinction offset calculated from a comparison of the brightness of stars within the image to those in the APASS DR7 and/or NOMAD public catalogs [26-27]. $t_{effective} = 1$ corresponds to an exposure taken at zenith with no moon, clear skies, and nominal seeing, and sky brightness, and atmospheric extinction. We require that $t_{effective} > 0.2$ for g, and Y-bands and $> 0.3$ for r, i, and z-bands. Each image is then checked for artifacts, such as satellites and airplane trails, and these images are flagged.

Supernovae are discovered by searching for temporal variations in brightness between SN exposures and SN template images of the same fields. These SN search images are first processed through a detrending pipeline similar to First Cut, and then through a difference imaging pipeline [23]. The SN difference imaging pipeline aligns the template and search images, adjusts the template image to match the seeing conditions of the search image, then subtracts the two images to produce a "differenced" image. Object detection software runs over the differenced image to identify transient objects, these transient objects are then passed through machine learning algorithms [28] to identify transients

which are supernova candidates. The data quality and the efficiency of this pipeline is monitored by inserting fake supernovae into the search images, and then monitoring how well these fake events are recovered by the pipeline. In particular, four fake supernovae of fixed magnitude (magnitude 20) are inserted into each CCD in each search image. The search images are considered to be of acceptable quality if > 90 % of the fixed magnitude fakes is recovered and the S/N ratio of the magnitude 20 fakes is > 20 for shallow fields and > 80 for deep fields. There is an additional requirement that seeing is < 2.0 arc seconds if projected to i-band at zenith instead of the filter/airmass combination of the exposure.

The First Cut processing and data quality evaluation and the SN image pipeline are typically turned around in less than 24 hours. The results are applied to the Exposure Table by the Run Manager as described previously.

## 3. CAMERA & TELESCOPE MAINTENANCE AND UPGRADES: Y4 TO Y5

Generally, the camera and telescope performance has been very good since Science Verification, which was during 2012. A continuous effort to improve has been carried-out by scientists and technical staff from CTIO and DES. We discussed those that occurred in 2012 to 2014 in the "DECam Paper" [5] and elsewhere [3,4]. We expect that CTIO staff will discuss improvements to the Blanco telescope slew time and dome positioning controls at this conference. There are a few items that we discuss in some detail here.

The first of these led to an improvement in the DECam image quality. It is helpful to describe how the DECam adaptive optics system (AOS) [5,29] works, for the system is transparent for the typical visiting astronomer, who doesn't have to take time optimizing the telescope focus by taking special exposures. The hexapod, which mechanically couples DECam to the Prime Focus Cage, provides position adjustment for DECam with 5 degrees of freedom with respect to the primary mirror: translation, piston, tip & tilt. A look-up-table (LUT) provides the nominal hexapod position as a function of temperature, Hour Angle, and Declination. The AOS then uses out-of-focus stars on CCDs located above and below the nominal focal plane to supply a position correction to the hexapod, based on analysis of the just-readout exposure, in time for the next one. This takes care of focus (piston) as well as coma correction. The improvement is that the out-of-focus stars now also provide a measure of the astigmatism in the exposure. The astigmatism can only be corrected by adjusting the shape of the Blanco Primary mirror. Taking advantage of improvements to the primary mirror air pad controls that were completed in 2014, DES & CTIO scientists developed a correction [30] to the air pad pressures that removes aberrations, particularly astigmatism, from the primary mirror shape. We have seen a slight improvement in the median PSF in Y4 and Y5 compared to previous seasons that may indicate an improvement of 0.2", to be taken in quadrature from a nominal PSF of typically ~0.9". To our knowledge, this is the first time that one of these thick, heavy (~17 ton) mirrors has been used this way.

The DECam focal plane is kept at operating temperature, -100C, by means of a liquid nitrogen ($LN_2$) system. A 200L tank resides on a platform in the dome, just to the side of the telescope. A pump, submerged in the tank, pumps 2 gallons of $LN_2$ per minute to a heat exchanger, connected to the back of the focal plane, within the DECam Dewar. The 100 PSI $LN_2$ is pumped up to the camera and returned in vacuum-jacketed pipes with total length of ~470 feet. The total heat-load should be < 500W. Two 300W compressed-He cryocoolers supply the refrigeration that re-liquifies the two-phase $N_2$ that is returned to the tank. For more details, see the DECam paper [5]. The cooling should be operable as a closed-system; that is, with the two cryocoolers able to supply sufficient refrigeration that no $N_2$ is lost. However, up to the end of Y4 we had not sustained that condition for long periods. The principal contributor to the extra heat load was a leak from one of the high-pressure N2 pipes into the vacuum jackets for the section of pipe that connected to the imager Dewar. During one period in July and August 2017, the vacuum in the supply line degraded from 0 to 250 mT in 25 days before the line was pumped out. Shortly after that we replaced the TEFLON gasket, which not only made the internal seal but also provided electrical isolation of the Dewar from the $N_2$ pipes, with a harder and tougher gasket made from VESPEL plastic. Later we made that change to the return line segment as well. In the meantime, experience with the system resulted in the development of a maintenance schedule for the cryo-coolers. With these changes the system has operated in closed-loop fashion for the past 9 months. There is a second issue with the $LN_2$ system. We continue to need to replace the submerged $LN_2$ pump. Discussed in detail in [5], the problem is the bearing cages that support the rotor shaft wear away. From Sept. 2012 to Aug. 2017 we used TEFLON cages impregnated with molybdenum disulfide, and we replaced the pumps after 8 to 9 months. In Aug. 2017 we tried VESPEL plastic bearing cages. That pump failed after ~5 months and we lost 2.5 nights of telescope time as a result.

We have retreated to the original design at CTIO and, at Fermilab, are currently testing the lifetime of PEEK cages coated with tungsten disulfide.

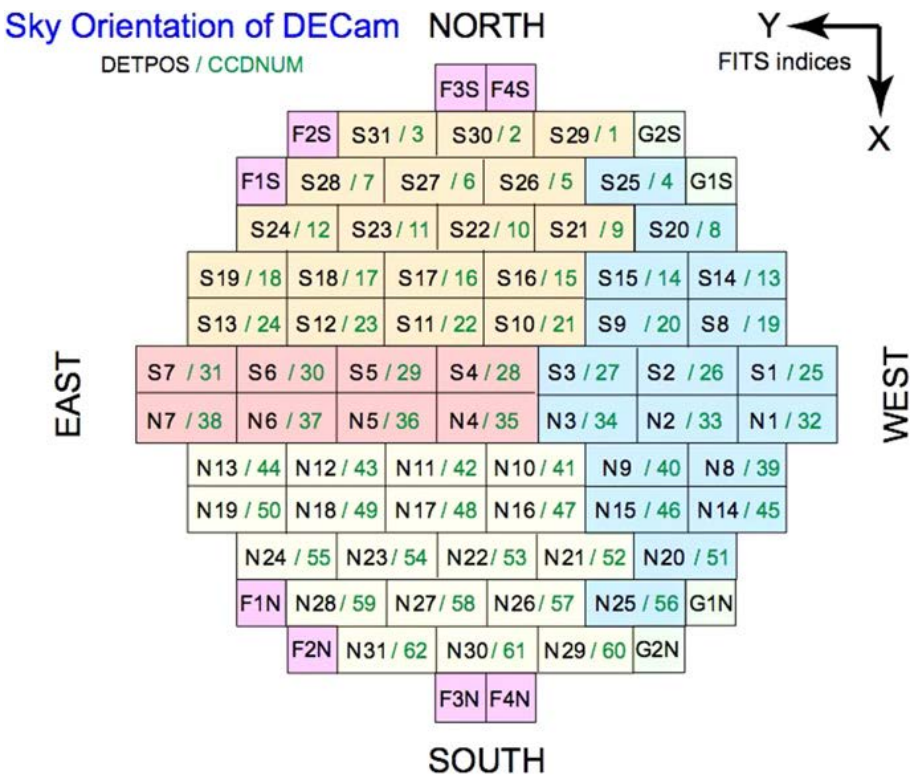


*Figure 4 DECam focal plane showing the 62 2k × 4k CCDs, 8 2k × 2k CCDs (labeled "F") for the adaptive optics system, and 4 2k × 2k CCDs (labeled "G") for guiding. The orientation of the sky is indicated. The label (e.g., S30) indicates a position on the focal plane. The label (e.g., 2) indicates the number of the CCD as is in the multi-extension FITS header. When the focal plane is viewed with the real-time display at the telescope or with default SAOImage DS9 settings, the direction labeled "north" is displayed to the left and "east" at the top. The background colors of the CCDs indicate the electronics backplane that reads them out. See Ref. [5] for details.*

The DECam focal plane has 62 2kx4k imaging CCDs, 4 2kx2k "Guide" CCDs and 8 2kx2k "alignment" CCDs, as is shown in Figure 4. These are in good working order except for CCD N30, which failed Nov. 7, 2012. Amplifier A of CCD S7 has an unpredictable time-varying gain and is not used for DES science. CCD S30 failed on Nov. 30, 2013 but, oddly, returned to good condition Dec. 29, 2016, 37 months later. We presume some material in the Dewar that had caused an amplifier ($V_{reset}$) short simply fell off. On Nov. 10, 2017, CCD N15 developed a "hot pixel" defect that requires masking out a small region. That problem largely disappeared by February 2018. Repairing these problems or replacing the problematic CCD's would require removing the Dewar from the camera. It is not planned to be done. A record of important events or changes to the camera or telescope is available online [31].

## 4. THE DES Y4 TO Y5 NARRATIVE, EFFICIENCY, LOSSES, AND PROGRESS

### 4.1 Survey Progress Prior to Y4

After DES seasons Y1 through Y3, we had fallen behind WF survey goals by 0.6 seasons, losing a tenth of a season in Y1 primarily due to problems with the Blanco environmental controls, a tenth of a seaon in Y2 primarily due to below average weather, and 4/10$^{ths}$ of a season in Y3 due to the worst weather in the 50 year history of CTIO [3,4]. That bad weather was due to a strong El Niño. Figure 5 shows the completion map for each of the five DES filters. We planned to have completed 6 tilings in each filter and wouldhave done so under "median" weather conditions.

You can see that we had completed only 4 to 5 tilings, except for the weat side in the Y-band filter. The DES Supernovae Surveys were interleaved with and were subject, of course, to the same conditions as the corresponding WF survey. The OBSTAC conditions protect the SN to some extent, by forcing re-observation of the SN fields if the previous night's images were of insufficient quality.

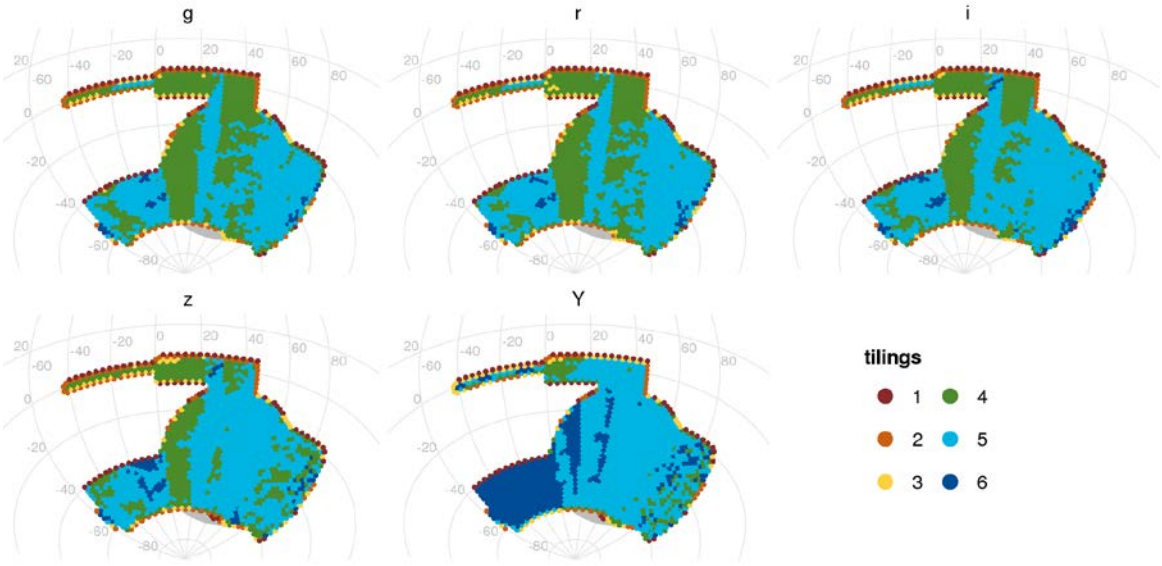


*Figure 5 The completed Y1-Y3 survey fields in each filter. The colored dots represent the number of "good" exposures. By the end of Y3, the WF survey is 6/10ths of a season short of where we planned for it to be under median weather conditions.*

**4.2 WF Survey Progress in Y4 & Y5**

Because of Y3's terrible weather, we became newly sensitized to long-term weather predictions and climate conditions. We learned that the Y3 El Niño was caused by the warmer than average temperature of the southern oceans, and it had been predicted by climate forecasters [32]. A few months before the start of Y4, the forecasts predicted neutral to La Niña conditions.

Y4 started on August 13, 2016 with 19 2nd half nights. We switched to full nights on Sept. 6, and switched to 1st half nights on Dec. 25, 2016. Table 2 shows the nominal start and end dates for Y1 through Y5 as well as the number of scheduled half-nights and full nights. The observing strategy was to complete at least two more tiles in each filter, with some priority given to finishing tiling 5, 6 and 7. The OBSTAC plan (see Section 2) for Y4 was to continue to ensure that exposures on the western side of the WF footprint were given sufficient priority at the beginning of the season, because that side of the footprint is already descending. Therefore, OBSTAC prioritized exposures west of R.A.=30 degrees by closeness to transit, and east of R.A.=30 degrees by setting time. In Y4 we dropped WF tilings 8 and 10 from the Y-band, instead increasing the tiling 7 & 9 exposure time from 45s to 90s. Finally, we made a slight adjustment to the SN survey start-up, whereby we initiated the individual SN fields deadman sequences only after the field was first observed under the OBSTAC poor-seeing condition.

We tracked the observing efficiency using a combination of information including the ELog, the DES and CTIO Night Reports, and other tools. The DES and CTIO Night Reports were collated to produce the estimate of how we spent our time. That is reported in Table 3. Y4 was much better than any of Y1 through Y3. The weather was generally good, with "Dome closed" conditions only 6.4% of the time, which is close to the historical median. The camera and telescope were reliable. The single biggest losses came from a power outage accompanied by a failure of the backup power system (cost one night), a problem with the hexapod recovery from the power outage (cost the next night), and an incident when the roughing pump that backs up the Dewar turbo pump failed, causing us to warm up the camera in case anything had frozen to the CCD surface (cost us a ½ night).

In Y4 we recorded 16,217 good exposures. A DES record 89.5% of the exposures were good by First Cut, compared to 78.7% for Y1 to Y3. Taking into account that many of these were Y-band tiling 7 or 9 (which should be counted as double), that goes to 17,211. A median season should provide 16,045 good exposures, two complete tilings, so we made up some of the previous losses. We finished tilings 5 and 6 and made good progress on tiling 7. Figure 6 shows the WF survey completion map after Y4.

*Table 2 Scheduled start and end dates for DES observing, and the number of half-nights and full nights for Y1 to Y5. Note that Y4 has 110 scheduled nights, instead of the usual 105. That is because we were expected to expend 5 nights on various TOO programs. Instead, we expended 2 nights. To make up for that, Y5 was scheduled for only 104 nights with one of those nights expected to be expended over a number of nights for a TOO. We did that TOO, as well as 30 hours on the DES-GW TOO. Those 30 hours were reimbursed to DES in February 2018, so that we ended up with 102 nights-equivalent for DES. *Four of the nights indicated as 1st half nights were ¾ nights long.*

| Season | Nominal Start Date | Nominal End Date | 2nd Half Nights | Full nights | 1st Half Nights |
|---|---|---|---|---|---|
| Y1 | Aug. 31, 2013 | Feb. 09, 2014 | 0 | 91 | 28 |
| Y2 | Aug. 15, 2014 | Feb. 15, 2015 | 10 | 80 | 41 |
| Y3 | Aug. 04, 2015 | Feb. 12, 2016 | 32 | 73 | 39 |
| Y4 | Aug. 13, 2016 | Feb. 18, 2017 | 19 | 76 | 49 |
| Y5 | Aug. 15, 2017 | Feb. 10, 2018 | 20 | 67 | 50* |

*Table 3 DES Operational efficiency sums accumulated through Y5. These are based on the observer's reports in the CTIO Night Summaries. "Time Available" is the time we should spend observing." Observing Time" is the number of hours the observers were actually engaged in observing. "Engineering Observations" are those in service to the understanding of camera or telescope systematics. Next is indicated the number of hours lost to bad weather that results in closing the dome instead of observing, to a failure of the telescope, dome, or mountaintop infrastructure, to the camera. *The Y1-Y3 weather loss is dominated by Y3, when we were "dome closed" for 294 hours (30.3%).*

| **Operations** | **DES Yr. 1-3 Averages Hrs. (%)** | **DES Yr. 4 Accumulated Hrs. (%)** | **DES Yr. 5 Accumulated Hrs. (%)** |
|---|---|---|---|
| Observing Time Available | 929 (100%) | 1011 ½ | 990 |
| Observing Time | 723 ½ (78%) | 912 ¾ (90.2%) | 908 ¾ (91.8%) |
| Engineering Observations & Other Losses | 1 ½ (<0.2%) | 2 (0.2%) | ¾ (0.1%) |
| Bad Weather | 174 2/3 (19%*) | 64 ¾ (6.4%) | 53.9 (5.4%) |
| Telescope or Infrastructure Failure | 16 1/3 (1.8%) | 18 ¼ (1.8%) | 5.4 (0.6%) |
| Camera Systems Failure | 13 (1.4%) | 13 ¾ (1.4%) | 21 ¼ (2.1%) |

Y5 started on August 15, 2017 with 2nd half night observing. We switched to full nights on Sept. 1st (with a half night and some ¾ nights thrown in here or there), and then to 1st half nights on Dec. 26, 2017. See Table 2. The climate forecasts [32] were neutral between El Niño and La Niña conditions. The observing strategy was to complete at least two more tiles in each filter, with some priority given to finishing tiling 7 and 8 and the hope that we would finish much of tiling 9, too. We used the same OBSTAC plan as Y4, noting that with the improved telescope slew time, we gave equal priority to any exposures with slew to <4 deg. In the past we had given higher priority to an exposure with no slew. To increase observing efficiency, we removed the thin part of Stripe 82 (west half around DEC = 0) from OBSTAC, preventing our making long slews back and forth between that part of Stripe 82 and the footprint further

south. We used standard observing scripts to observe that part of Stripe 82. For similar reasons, all other things being equal, OBSTAC preferred exposures with a slew in RA over a slew in DEC.

As is reported in Table 3, Y5 was great. The weather was in the historical top quartile [5], with "Dome closed" conditions only 5.4% of the time. The telescope was reliable. The camera had one serious downtime incident, in December 2017, when the submerged $LN_2$ pump failed (see Section 3, VESPEL bearing cages). DES lost 2.5 nights before the spare pump was installed and the camera re-cooled to operating temperature. Otherwise, DES was on the sky for 91.8% of the observing time, a record for DES. When we were observing, the shutter was open 68.5% of the time, also a record for DES, presumably due in part to improvements in the telescope slewing and dome controls mentioned in Section 3, as well as the efforts to improve the survey efficiency through adjustments to OBSTAC as is discussed above. Second only to Y4, 86.8% of the exposures were graded good by First Cut.

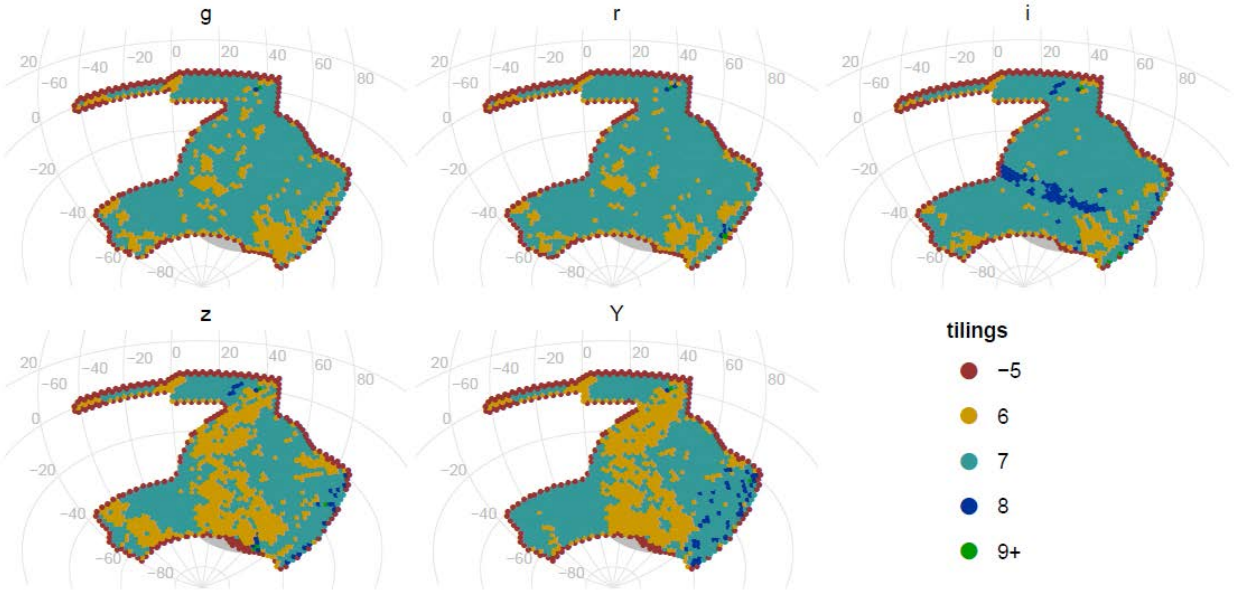


*Figure 6 The WF survey completion map at the end of Y4. Given median weather conditions for the survey, by the end of Y4 should have finished 8 tilings. Instead we've finished 6 to 7. The blue stripes (8 tilings completed) in the i-band corresponds to where a TOO that required 90s exposures coincided with the DES footprint.*

In Y5 we recorded 15,212 good exposures. Taking into account that many of these were Y-band tiling 7 or 9 (which should be counted as double), that goes to 16,486, just a bit better than the expected median season, but in only 102 nights. We finished tiling 7, almost all of tiling 8 (except for the skinny part of Stripe 82 in the Y-band), and much of tiling 9 in all filters. Much of the west side of the Y-band is completed, as is a part of the i-band. Figure 7 shows the WF survey completion map after Y5.

DES science requirements, particularly the weak lensing shear analyses [33], put a premium value on good point-spread-function (PSF) for the r,i, and z-band exposures. The Y4 and Y5 data meets that standard. Y5 has the best achieved PSF of any DES season. Figure 8 shows the PSF for WF images in all 5 filters for Y4 and Y5.

### 4.3 Target of Opportunity Observing

DES made arrangements with CTIO and two external groups that provided for "Target of Opportunity" (TOO) observing time during nights that DES was observing. In case of the need for such observations, the external group contacted DES operations, and provided the observing scripts and the order and conditions under which they were to be executed. The external groups shared weather risk with DES. The total time that was used for TOO's was tracked. In Y4 5 extra nights were planned for TOOs and "pre-imbursed" to DES. "DES-GW" (PI-Berger) searched for optical counterparts to LIGO/VIRGO triggers [34], and used only two night-equivalents.

The Y5 TOO programs were "DES-GW" (PI-Berger), again searching for optical counterparts to LIGO/VIRGO triggers, and "DES-IC" (PI-Bechtol), which sought optical counterparts to energetic neutrino triggers from ICE-CUBE [35]. DES-GW was particularly active, successful, and indeed exciting. The excitement started on the night before

the official start of the survey with LIGO/VIRGO GW170814, a binary black hole collision wholly in the DES footprint. Just a few nights later LIGO/Virgo trigger GW170817 was announced. Of course, that is now famous, as it immediately led, within hours, to discovery of the optical counterpart of binary neutron star system, and DES shares a part of the discovery [36]. An array of remote stations set up at Fermilab in the "Neutrino Remote Operations Center" (νROC) was sometimes used to participate in and assist with the TOO observations that were going on at CTIO. DES observers smoothly handled more than 40 TOO interruptions of OBSTAC in Y5.

### 4.4 Y4 & Y5 SN Surveys

We carried out the DES supernova survey in Y4 and Y5. The SN survey consumed 30% of the exposure time. Figure 9 shows the nights on which we observed each SN sequence for the 10 SN fields. The full set of SN exposures takes 8 ½ to 9 hours. There are 16 SN sequences (8 shallow fields with g,r,i, & z-bands in the sequence, and 2 deep fields each with separate g, r, i, and z-band sequences). See Section 1. We successfully observed all 16 SN sequences in a single night twice in Y2 and once in Y5. Gaps between observations of a given field are due to bad weather (rather rare in Y4 and Y5), to holes in the DES schedule, or (worst) to the combination of the two where we have only a few nights in a single stretch to observe all 15 sequences. In Y4 and Y5, 30% of the observing time was for used for SN observations. During Y1 through Y3, there was an average of 21.6 good sets of observations for each of the 16 sequences. During Y4 that increased to 25.9. In Y5, that fell slightly, to 24.2 good sets, only because we ended some of the SN sequences about two weeks earlier than we did in previous years, due to uncertainty in the schedule that suggested we raise the priority of the WF survey. The DES SN survey ended with the end of Y5.

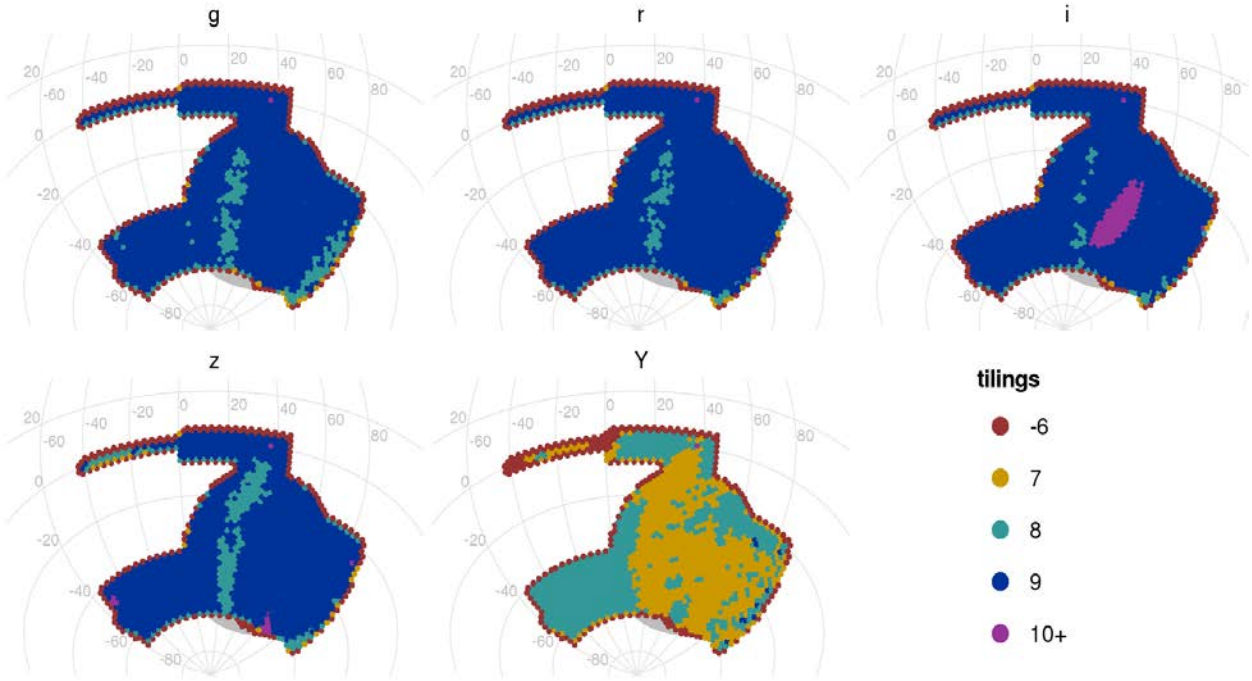


*Figure 7 The WF survey completion map at the end of Y5. Given median weather conditions for the survey, by the end of Y4 should have finished the full 10 tilings of the survey. Instead we've finished 9, averaged over the five filters. Some areas are complete (see purple regions for g,r,i & z-band and light blue for Y-band). The completed region in the i-band corresponds to where a TOO that required 90s exposures coincided with the DES footprint.*

### 4.5 Additional Special Purpose Fields Observed in Y4 & Y5

We used DES time to take some special observations in Y4 and Y5. In order to provide a cross check of the DES photometric redshift methodology we observed the ALH-2/DEEP2, ALH-8/SDSS, and COSMOS fields [37-38] to at least DES depth in ugrizY filters under photometric observing conditions with median PSF and low airmass. We took short duration exposures of white dwarf spectrophotometric standard stars LDS749B/HST and WD0308-565/HST [39] to cross check our photometric calibration.

In addition, during Y5 we took special observations of five nearby, confirmed Type1a SN. These exposure sequences were 30s in each of u, g, r, i, and z-bands. The sequences were repeated 10 times over a duration of about a month. The purpose of these observations was to provide an anchor to the low-redshift end of the Hubble diagram. During a prior season we observed all each of the DES SN fields in u-band for 55 minutes.

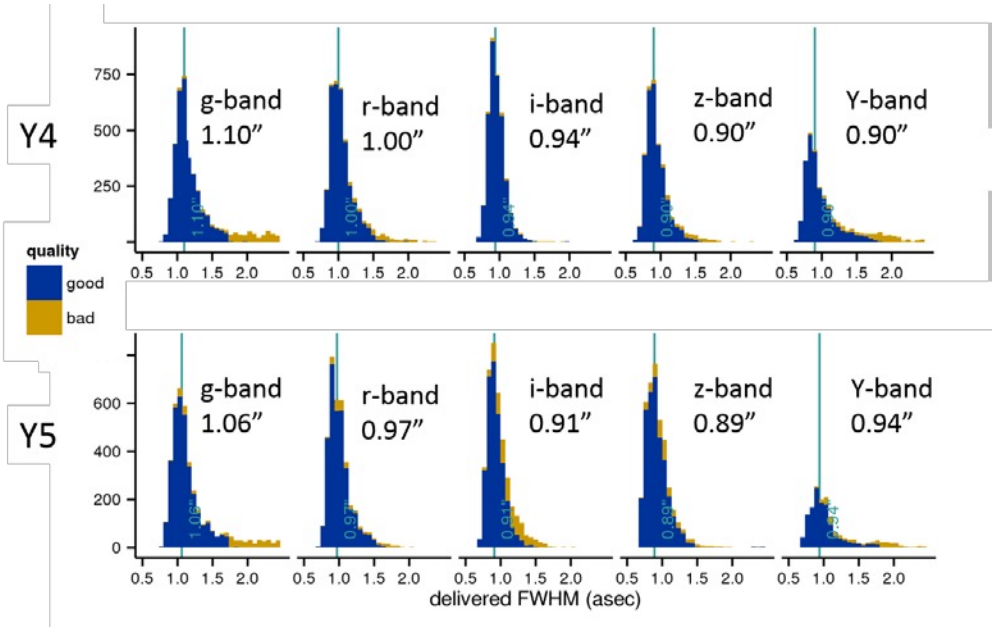


*Figure 8 The "point-spread-function" (PSF), full-width half-max, of Y4 and Y5 DES WF survey exposures. The quality "good" or "bad" is the result of First Cut, discussed in Section 2.*

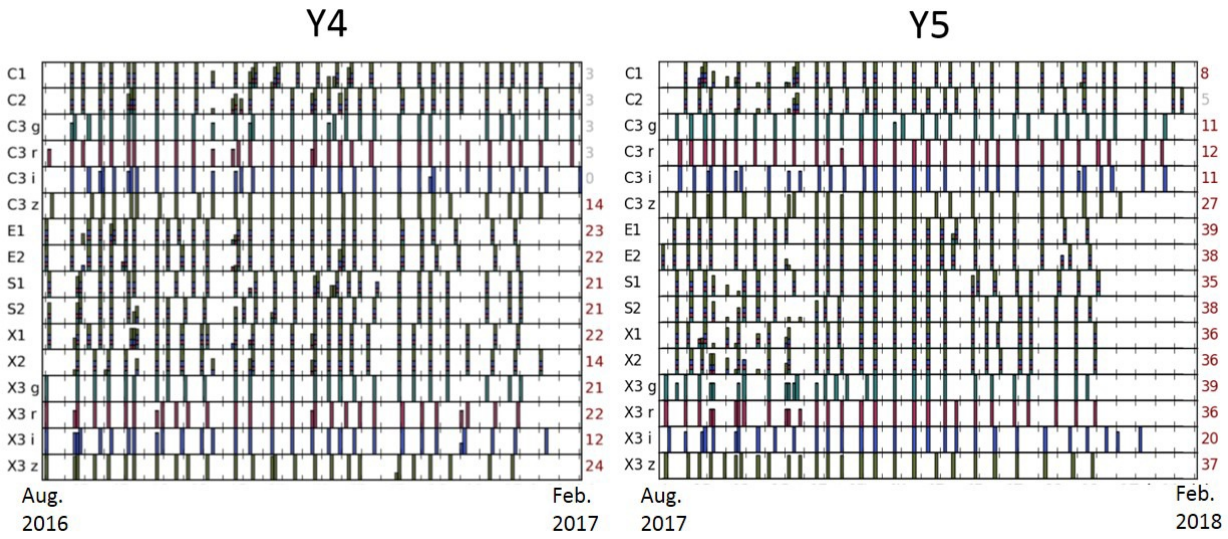


*Figure 9 The DES Yearly SN observations, good data only, Y4 and Y5. The horizontal axis is the date from the beginning of the season to the end of the season (see Table 2 for precise dates). The vertical axis lists each of the 10 SN fields. If the SN field was observed there is a vertical bar with a separate color block for each filter. The two "deep fields" are C3 and X3.*

## 5. SURVEY SEASON Y6 AND OUTLOOK

DES has proposed to successfully complete the ten tilings of the 5000 sq-deg WF survey and our funding agencies and stakeholders have agreed. The Y6 observing season is expected to start in early September 2018. With only 52 nights, a half-season, DES will finish in late-December 2018. Schedule details aren't available as of this time. The goal for WF observing will be to complete the WF survey. We are hoping that Y6 is at least a median weather season. Simulation indicates that if the weather is median or better, we will complete the ten tilings. The climate forecasts indicate [32] a slight preference for a weak El Niño during the Y6 observing season, but with low confidence.

In between Y5 and Y6 CTIO will resurface the Blanco Telescope primary mirror with a fresh aluminum coating. This was most recently done in 2011. CTIO will perform routine maintenance will occur on the camera cooling system and the filter changer, which needs replacement of the insertion/removal air cylinder for at least one filter position. See Ref. [5] for design information.

We will start Y6 observations on the west side of the survey field, occasionally giving priority to tiling 9 over tiling 10. As we did in Y5 to optimize survey efficiency, we will observe the thin part of Stripe 82 only using observing scripts. For the first time, DES will not carry out the SN survey, simplifying the OBSTAC flowchart of Figure 3. In previous seasons we took SN exposures when the seeing was poor (in range i-band, projected to zenith 1.1" to 2.0"). We found that if the seeing is worse than 1.6" or 1.7" (i-band projected to zenith), the OBSTAC "condition 4" WF g- and Y-band exposures usually don't pass data First Cut data quality. We are considering ideas generated within the collaboration including, for instance, observing the SN fields in Y-band to improve photometric redshifts. We expect roughly 5% of the time will be in this condition. As the season progresses and we measure our progress, we will adjust our observing priorities to insure we have as complete a WF survey as possible. Depending on how we are doing, that could mean skipping over parts of the WF where we have already done very well in previous seasons (in summed $t_{eff}$, for instance), or perhaps adding extra exposures (in case we get ahead of the simulation) to where the survey is a bit shallower.

There are no plans for DES Y7 observations. After DES, the DECam will continue to be available as a Community Instrument on the Blanco Telescope for a long time.

## 6. SUMMARY

The Dark Energy Survey Collaboration studies the accelerating expansion of the Universe through four complementary techniques. To produce the deep, 5000 square-degree survey and the 30 square-degree time-domain SN survey that are specified by the science goals, the collaboration designed and built the Dark Energy Camera, now operating on the Blanco Telescope at CTIO. We have finished the first 5 seasons. Operational procedures have been effective in making good use of our observation time. Our survey efficiency was highest in Y5, in part due to improvements. However, primarily because of extremely poor weather in Y3, we are only 90% complete after the nominal planned end of the survey. Therefore, we petitioned-for and received an extra half-season of 52 night-equivalents. DES Y6 is expected to start in early September 2018 and to finish in late December. In a median weather Y6 season, we will finish observations of the 10 tilings in all 5 filters, completing the original DES survey goals.

In Jan. 2018, the collaboration put out its first major public data release, DR1 (Dark Energy Survey Collaboration 2018). Based on data from the first 3 years of the survey, it comprises reduced single-epoch images, co-added images covering the full 5000 $deg^2$ survey footprint and catalog information for 400 million objects [40]. It has a photometric precision of < 1% in all bands, and an astrometric precision of 151 mas. The median coadded catalog depth for a 1.95" diameter aperture at S/N = 10 is g = 24.33, r = 24.08, i = 23.44, z = 22.69, and Y = 21.44 mag. Access to this data is via a range of interfaces, including query web clients, image cutout servers, jupyter notebooks and an interactive coadd image visualization tool. DES DR1 constitutes the largest photometric data set to date at the achieved depth and photometric precision. We anticipate that it will be widely used by the astronomy community for a variety of studies; in the 5 months since the release, over 359 community users submitted over 2026 query jobs and generated ~3.8 Tb of user data.

The DES Collaboration has been working towards accomplishing the science goals. A series of publications describes and culminates [41] in DES's first significant cosmology results using the weak gravitational lensing technique. Using

the Y1 data alone, ~1500 sq. deq., we produced constraints on the growth rate of structure and the matter density, $\Omega_{m,}$ that compete with the world's previous best. It also includes limits on the dark energy equation of state parameter, *w*, and on the sum of the neutrino masses. The DES SN team produced preliminary cosmology results from the Hubble diagram of a sample of 334 spectroscopically confirmed SNe Ia (206 from DES to z=0.85, plus 128 from external, low-z samples) from Y1-Y3 data. With uncertainties smaller than those from some larger, recent SN samples, due to improved control of systematic errors, we produce competitive constrains on *w* and $\Omega_m$ [42]. Cosmology results based on Y1 data from the large scale structure (BAO) are consistent [43] with the other DES cosmology measurements. Cosmological constraints from galaxy abundances are imminent.

The many papers span topics from extra-galactic astrophysics, to studies of the Milky Way, to the discovery of objects in our solar system. Among the highlights in the past year are the discovery [44] of eleven new stellar streams around the Milky Way as well as extra-tidal stellar structure associated with four known globular clusters, and continued study of DES-discovered [45-46] Milky Way dwarf galaxies. DES produced [47] a precise measurement of $H_0$ from DES Y1 WL result combined with BAO, and D/H data. DES presented the discovery of hundreds of bright strong-lensed (SL) galaxy candidates in the SV and Y1 data [48], new quadrupole and binary SL quasar systems [49], and a time delay measurement from our previously reported quadruply-lensed quasar system DESJ0408-5354 [50]. Solar system results include the discovery of the 2nd-most distant trans-Neptunian object [51]. As of mid-spring 2018 (northern hemisphere), the DES Collaboration has 122 accepted and/or published refereed science papers with 45 more submitted and under referee review. We cannot remark on all of them. It is obvious from the number and scope of our publications that DES is already a successful survey and we look forward to producing even more important results in the near future.

## 7. ACKNOWLEDGEMENTS

We are grateful for the extraordinary contributions of our CTIO colleagues and the DES Camera and Operations Support teams in achieving the excellent instrument and telescope conditions that have made this work possible. We are grateful for the administrative and organizational assistance provided by Connie Lang (FNAL) and Ximena Herreros (CTIO).

Funding for the DES Projects has been provided by the U.S. Department of Energy, the U.S. National Science Foundation, the Ministry of Science and Education of Spain, the Science and Technology Facilities Council of the United Kingdom, the Higher Education Funding Council for England, the National Center for Supercomputing Applications at the University of Illinois at Urbana-Champaign, the Kavli Institute of Cosmological Physics at the University of Chicago, the Center for Cosmology and Astro-Particle Physics at the Ohio State University, the Mitchell Institute for Fundamental Physics and Astronomy at Texas A&M University, Financiadora de Estudos e Projetos, Fundação Carlos Chagas Filho de Amparo à Pesquisa do Estado do Rio de Janeiro, Conselho Nacional de Desenvolvimento Científico e Tecnológico and the Ministério da Ciência, Tecnologia e Inovação, the Deutsche Forschungsgemeinschaft and the Collaborating Institutions in the Dark Energy Survey.

The Collaborating Institutions are Argonne National Laboratory, the University of California at Santa Cruz, the University of Cambridge, Centro de Investigaciones Energéticas, Medioambientales y Tecnológicas-Madrid, the University of Chicago, University College London, the DES-Brazil Consortium, the University of Edinburgh, the Eidgenössische Technische Hochschule (ETH) Zürich, Fermi National Accelerator Laboratory, the University of Illinois at Urbana-Champaign, the Institut de Ciencies de l'Espai (IEEC/CSIC), the Institut de Física d'Altes Energies, Lawrence Berkeley National Laboratory, the Ludwig-Maximilians Universität München and the associated Excellence Cluster Universe, the University of Michigan, the National Optical Astronomy Observatory, the University of Nottingham, The Ohio State University, the University of Pennsylvania, the University of Portsmouth, SLAC National Accelerator Laboratory, Stanford University, the University of Sussex, Texas A&M University, and the OzDES Membership Consortium.

Based in part on observations at Cerro Tololo Inter-American Observatory, National Optical Astronomy Observatory, which is operated by the Association of Universities for Research in Astronomy (AURA) under a cooperative agreement with the National Science Foundation.

The DES data management system is supported by the National Science Foundation under Grant Numbers AST-1138766 and AST-1536171. The DES participants from Spanish institutions are partially supported by MINECO under grants AYA2015-71825, ESP2015-66861, FPA2015-68048, SEV-2016-0588, SEV-2016-0597, and MDM-2015-0509, some of which include ERDF funds from the European Union. IFAE is partially funded by the CERCA program of the Generalitat de Catalunya. Research leading to these results has received funding from the European Research Council under the European Union's Seventh Framework Program (FP7/2007-2013) including ERC grant agreements 240672, 291329, and 306478. We acknowledge support from the Australian Research Council Centre of Excellence for All-sky Astrophysics (CAASTRO), through project number CE110001020, and the Brazilian Instituto Nacional de Ciencia e Tecnologia (INCT) e-Universe (CNPq grant 465376/2014-2).



## REFERENCES

[1] Flaugher, B., "The Dark Energy Survey", Int. J. Modern. Phys. A20, 3121 (2005).
[2] Dark Energy Survey Collaboration, "The Dark Energy Survey: more than dark energy - an overview", MNRAS 460 1270 (2016).
[3] Diehl, H. T. et al., "Dark Energy Survey Operations: Year 1", Proc. SPIE 9149, 91490V (2014).
[4] Diehl, H. T. et al., "Dark Energy Survey Operations: Years 1 to 3", Proc. SPIE 9910, 99101D (2016).
[5] Flaugher, B., Diehl, H. T., Honscheid, K. et al., "The Dark Energy Camera", AJ 150, 150 (2015).
[6] Lewis, P. M., Rogers, H., & Schindler, R. H., "A radiometric all-sky infrared camera (RASICAM) for DES/CTIO", Proc. SPIE, 7735, 77353C (2010)
[7] Reil, K., Lewis, P., Schindler, R. H., & Zhang, Z., "An update on the status and performance of the Radiometric All-Sky Infrared Camera (RASICAM)", Proc. SPIE, 9149, 91490U (2014)
[8] Blake, C. H., & Shaw, M. M. 2011, PASP, 123, 1302.
[9] Li, T., DePoy, D. L., Kessler, R. et al., "aTmcam: a simple atmospheric transmission monitoring camera for sub 1% photometric precision", Proc. SPIE, 8446, 84462L (2012)
[10] Li, T., DePoy, D. L., Marshall, J. L. et al., "Monitoring the atmospheric throughput at Cerro Tololo Inter-American Observatory with aTmCam", Proc. SPIE, 9147, 91476Z (2014)
[11] Ruhl, J. E., et al., "The South Pole Telescope", Proc. SPIE 5498, 5498-11 (2004).
[12] L. Jiang et al., "The Sloan Digital Sky Survey STRIPE 82 Imaging Data: Depth-optimized co-adds over 300 deg$^2$ in five filters", ApJS 213, 12 (2014).
[13] Kessler, R., Marriner, J., Childress, M., et al., "The Difference Imaging Pipeline for the Transient Search in the Dark Energy Survey", AJ 150, 172 (2015).
[14] See URL https://cdcvs.fnal.gov/redmine/projects/desops/wiki
[15] Rheault, J.-P., Depoy, D. L., Marshall, J. L., et al., "Spectrophotometric calibration system for DECam", Proc. SPIE 8446, 84466M (2012).
[16] Tucker, D. L., et al., in ASP Conf. Ser. Vol. 364, The Future of Photometric, Spectrophotometric and Polarimetric Standardization, Astron. Soc. Pac., ed. Sterken C., San Francisco, 187 (2007).
[17] Fitzpatrick, M. J., "DTS: The NOAO Data Transport System", Proc. SPIE 7737, 77371T (2010).
[18] http://portal-nvo.noao.edu
[19] Pence, W. D., Seaman, R., & White, R. L., "Lossless Astronomical Image Compression and the Effects of Noise", PASP 121, 414 (2009) and http://heasarc.nasa.gov/fitsio/fpack.
[20] Smith, R. C., Walker, A. R., and Miller, C., "DECam Community Pipeline Software requirements and technical Specifications", http://www.noao.edu/meetings/decam/media/community_pipeline.pdf.
[21] Pence, W. D., White, R. L., & Seaman, R., "Optimal Compression of Floating-point Astronomical Images without Significant Loss of Information", PASP 122, 1065 (2010).
[22] Neilsen, E., and Annis, J., "OBSTAC: automated execution of Dark Energy Survey observing tactics", FERMILAB-CONF-13-397-CD.

[23] Morganson, E. et al., "The Dark Energy Survey Image Processing Pipeline", arXiv:1801.03177.
[24] Zacharias, N., et al., "The Fourth US Naval Observatory CCD Astrograph Catalog (UCAC4)" AJ **145**, 44 (2013).
[25] Neilsen, E., Bernstein, G., Gruendl, R., and Kent, S., "Limiting magnitude, τ, teff, and image quality in DES Year 1", FERMILAB-TM-2610-AE-CD (2015).
[26] Hendon, A. A., et al., JAAVSO **40**, 430 (2012) and http://www.aavso.org/apass.
[27] http://www.ap-i.net/skychart/en/news/nomad.
[28] Goldstein, D. A., D'Andrea, C. B., Fischer, J. A., et al., "Automated Transient Identification in the Dark Energy Survey", AJ 150, 82 (2015).
[29] Roodman, A., "Focus and alignment of the Dark Energy Camera using out-of-focus stars", Proc. SPIE 8446, 84466O (2012).
[30] Roodman, A. J., Reil, K., Davis, C., "Wavefront sensing and the active optics system of the Dark Energy Camera", Proc. SPIE 9145, 914516 (2014).
[31] https://cdcvs.fnal.gov/redmine/projects/desops/wiki/Log_of_Configuration_Changes
[32] http://iri.columbia.edu/our-expertise/climate/forecasts/enso/current/
[33] Zuntz, J. et al., "Dark Energy Survey Year 1 Results: Weak Lensing Shape Catalogues", arXiv:1708.01533, submitted.
[34] Soares-Santos, M. et al., "A Dark Energy Camera Search for an Optical Counterpart to the First Advanced LIGO Gravitational Wave Event GW150914", ApJ 823, L33 (2016).
[35] https://icecube.wisc.edu/
[36] Soares-Santos, M. et al., "The Electromagnetic Counterpart of the Binary Neutron Star Merger LIGO/Virgo GW170817. I. Dark Energy Camera Discovery of the Optical Counterpart", ApJ 848, L16, (2017).
[37] Refalh Povic, M. et al, "The ALHAMBRA survey: reliable morphological catalogue of 22051 early- and late-type galaxies", MNRAS 435, 3444–3461 (2013)
[38] http://cosmos.astro.caltech.edu/page/astronomers
[39] http://www.stsci.edu/hst/observatory/crds/calspec.html
[40] Abbott, T. M. C. et al., "The Dark Energy Survey Data Release 1", arXiv:1801.03181, submitted.
[41] DES Collaboration, Abbott, T. M. C. et al., "Dark Energy Survey Year 1 Results: Cosmological Constraints from Galaxy Clustering and Weak Lensing", arXiv:1708.01530, submitted.
[42] Brout, D. for the DES Collaboration, "Cosmological Parameter Constraints from the Dark Energy Survey Supernova Program Three Year Spectroscopic Sample", http://adsabs.harvard.edu/abs/2018AAS...23121904B.
[43] DES Collaboration, Abbott, T. M. C. et al., "Dark Energy Survey Year 1 Results: Measurement of the Baryon Acoustic Oscillation scale in the distribution of galaxies to redshift 1", arXiv:1712.06209, submitted.
[44] Shipp, N. et al., "Stellar Streams Discovered in the Dark Energy Survey", arXiv:1801.03097, submitted.
[45] Bechtol, K. et al, "Eight New Milky Way Companions Discovered in First-Year Dark Energy Survey Data", ApJ 807, 50 (2015).
[46] Drlica-Wagner, A. et al., "Eight Ultra-faint Galaxy Candidates Discovered in Year Two of the Dark Energy Survey", ApJ 813, 109 (2015).
[47] DES Collaboration, Abbott, T. M. C. et al., "Dark Energy Survey Year 1 Results: A Precise $H_0$ Measurement from DES Y1, BAO, and D/H Data", arXiv:1711.00403, submitted.
[48] Diehl, H. T. et al., "The DES Bright Arcs Survey: Hundreds of Candidate Strongly Lensed Galaxy Systems from the Dark Energy Survey Science Verification and Year 1 Observations", ApJS 232, 15 (2017).
[49] Agnello, A. et al., "DES meets Gaia: discovery of strongly lensed quasars from a multiplet search", arXiv:1711.03971, submitted.
[50] Courbin, F. et al, "COSMOGRAIL XVI: Time Delays for the Quadruply Imaged Quasar DES J0408-5354 With High-cadence Photometric Monitoring", A&A 609, A71 (2018).
[51] Gerdes, D. et al., "Discovery and Physical Characterization of a Large Scattered Disk Object at 92 AU", ApJ 839, L15 (2017).